Sliding Modes Applications in Power Electronics and Electrical Drives

Asif Šabanović[1], Karel Jezernik[2], and Nadira Šabanović[1]

[1] Sabanci University, Faculty of Engineering and Natural Sciences Orhanli, 81474 Istanbul-Tuzla, Turkey, e-mail: asif@sabanciuniv.edu.tr
[2] University of Maribor, Faculty of Electrical Engineering and Computer Science Smetanova ul. 17, SI-2000 Maribor, Slovenia, e-mail: karel.jezernik@uni-mb.si

Abstract. Control system design of switching power converters and electrical machines based on the sliding mode approach is presented. The structural similarities among switching converters and electrical machines are used to show that the same structure of the controller could be used for plants under consideration. The controller is designed as a cascade structure with inner current loop designed as a sliding mode system with discontinuous control and outer loop (voltage or mechanical motion) being designed as a discrete-time sliding mode controller.

1 Introduction

The aim of this paper is to present an application of sliding mode control in switching power converters and electrical drives. Our intention is to show that, due to the structural similarities, switching power converters and electrical machines could be analysed in the same framework and that the structure of the control system is the same for both plants. The basis for our approach is the analysis of switching converters and electrical machines as the set of energy storage elements with their interconnections dynamically changed by the operation of the switching matrix [2]. The switching matrix plays the role of a control element determining the power exchange between energy storing elements, introducing change in the structure of the system and, thus making design in the framework of variable structure systems and sliding mode control [1] a natural choice. Engineering methods rather than a historical overview of published results will be presented.

A functional description of switching power converters and electrical machines is presented in section 2. As a result of this analysis mathematical description that treats both converters and machines is devised and a formulation of the converters and electrical drive control, in the framework of VSS is derived. In the third section some results of VSS theory that are used in this paper are reviewed and the control algorithms common in switching converters and electrical machines control are discussed. In the same section design of voltage and power flow control for power converters and design of the motion control of electrical machines is presented. In the forth section the design of IM observer is discussed in details. The last section presents

experimental example of the neural network realisation of the sliding mode system for induction machine control.

2   Functional description of switching power converters and electrical machines

The role of the power converter is to modulate electrical power flow between power sources (Fig. 1). In general power flow can be bi-directional so both sources may the play role of power generator or power sink (load). The converter should enable that interaction of any input source to any output source of the power systems. It acts as a link having matrix-like structure. Efficient modulation of power flow is realised using switch-like elements having zero voltage drop when conducting and fully blocks current flow when open. Use of switches as structural elements of a converter offers opportunity to consider a converter as switching matrix. Disregarding the wide variety of designs in most switching converters, control of power flow is accomplished by varying the length of time intervals for which one or more energy storage elements are connected to or disconnected from the energy sources. Due to the restriction imposed by Kirchoff's circuit laws the nature of sources at zhe input and output sides of the switching matrix must be different (voltage or current sources)[2].

For purposes of mathematical modelling the operation of a switch may be described by a two-valued variable $u_{ik}(t), (i = 1, ..., n; k = 1, ..., m)$, having value 0 when the switch is open and value 1 when the switch is closed with average value $0 \leq \tilde{u}_{ik}(t) \leq 1$. If voltage sources are connected to input side of the switching matrix then restrictions imposed due to Kirchoff's circuit laws allow only one switch connecting one of the n input lines to the $k-$th $(k = 1, ..., m)$ output line can be closed during any time interval, or mathematically $\sum_{1=1}^{n} u_{ik}(t) = 1, k = 1, ..., m$. Allowed connections will be referred as permissible combinations.

An analogous requirement can be derived if the current source is attached at the input side of the switching matrix. The operation of the switching matrix changes the connections among elements of the switching converter
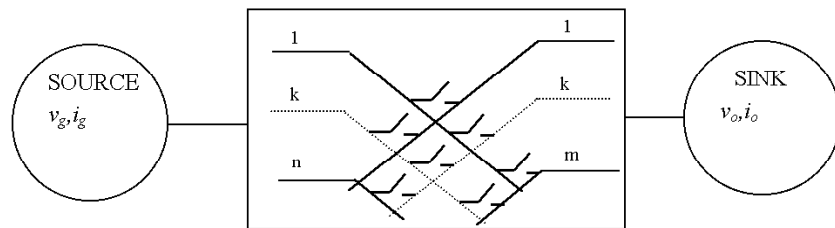

Fig. 1. Converter as a connection between power sources in a switching matrix connecting n-dimensional input and m-dimensional output.

and introduces variation in the dynamical structure of the system. Since the role of switching matrix is to control power flow, the most natural way to model the matrix is by introducing a control vector that will represent the effect of the matrix operation. Let the state of the switches be defined by the vector $\boldsymbol{s}_{sw}^{T} = [u_{11} \, .. \, u_{ik} \, .. \, u_{nm}]$ whose elements are two-valued variables $u_{ik}(t), (i = 1, ...n; k = 1, ..., m)$ describing the state of switches in each node of the switching matrix [3],[4]. The topological connection of the switches in the switching matrix is defined by the matrix $\boldsymbol{A}_M$ with elements being from the discrete set $S_3 = \{1, 0, -1\}$. The topological connection of the load with respect to the switching matrix defines the relations of the variables at the output lines of the switching matrix to the load quantities and could be defined by matrix $\boldsymbol{A}_L$. The operation of the switching matrix can be expressed by vector $\boldsymbol{u} = \boldsymbol{A}_M \boldsymbol{s}_{sw}$. Vector $\boldsymbol{u}$ has a number of distinctive values equal to the number of permissible switch connection.

2.1   Common converters and their operational properties

In Table 1 topological structure of the most common converters having voltage or current sources on input or output sides are depicted with transformation of variables. The simplest matrix - representing DC-to-DC converters - has only two switches interconnecting two unipolar sources. If unipolar and bipolar sources are to be interconnected then the switching matrix must have at least four switches. If one of the sources to be interconnected is three-phase then the structure has three output or three input lines, depending on the position of the AC source. These structures are representing three phase inverters (DC source at input side) and rectifiers (three phase source at input side).

The role of energy storing elements (L,C) is to balance power flow between source and sink by temporarily storage and release of energy [2]. The dynamics of converters depends on the topological relation of the energy storage elements to the switching matrix. Further analysis will be concentrate on two generic structures - both with inductance energy transfer. In the first - so called buck structure - inductance is connected to the output of the switching matrix, energy flow from the source is pulsating being modulated by the switching matrix. In the other - so called boost structure - inductance is connected to the source and the energy flow from the source is continuous while the switching matrix is modulating discontinuous energy flow to the output side.

Dynamics of DC-to-DC converters. Buck and boost structures of DC-to-DC power converters are shown in Table 2 along with their mathematical models. In the buck structure the dynamical structure of the system remains the same - an LC filter is connected to the variable source. In the case of the boost converter the dynamical structure is changed depending on the

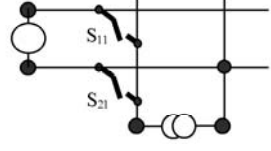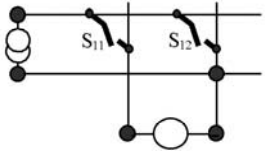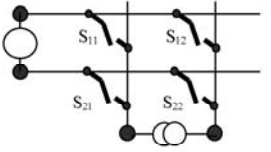**Table 1.** Topological structure of the most common switching matrices and their functional characteristics.
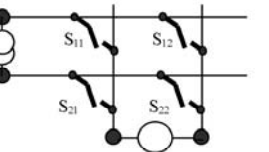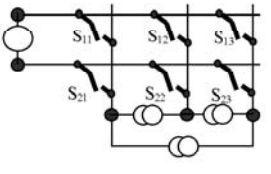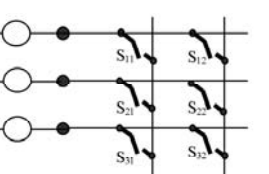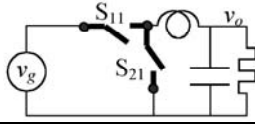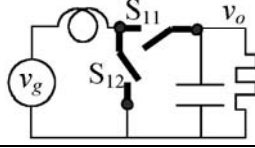
DC-to-DC converters		
Buck structure	Common relations	Boost structure
$v_s = v_g \boldsymbol{A}_L \boldsymbol{u}$ $\boldsymbol{u} = \boldsymbol{A}_M \boldsymbol{s}_{sw}$	$\boldsymbol{A}_L = [1]$ $\boldsymbol{A}_M = [1\ 0]$ $\boldsymbol{s}_{sw} = [u_{11}\ u_{21}]^T$	$i_s = i_g \boldsymbol{A}_L \boldsymbol{u}$ $\boldsymbol{u} = \boldsymbol{A}_M \boldsymbol{s}_{sw}$
DC-to-AC and AC-to-DC single phase converter		
Buck structure	Common relations	Boost structure
$v_s = \dfrac{1}{2} v_g \boldsymbol{A}_L \boldsymbol{u}$ $\boldsymbol{u} = \boldsymbol{A}_M \boldsymbol{s}_{sw}$	$\boldsymbol{A}_L = [1\ -1]$ $\boldsymbol{A}_M = \begin{bmatrix} 1 & 0 & -1 & 0 \\ 0 & 1 & 0 & -1 \end{bmatrix}$ $\boldsymbol{s}_{sw} = [u_{11}\ u_{12}\ u_{21}\ u_{22}]^T$	$i_s = i_g \boldsymbol{A}_L \boldsymbol{u}$ $\boldsymbol{u} = \boldsymbol{A}_M \boldsymbol{s}_{sw}$
Three phase converters		
Inverters	Common relations	Rectifiers
$v_s = \dfrac{1}{2} v_g \boldsymbol{A}_L \boldsymbol{u}$ $\boldsymbol{u} = \boldsymbol{A}_M \boldsymbol{s}_{sw}$ $\boldsymbol{A}_L = \begin{bmatrix} 1 & -1 & 0 \\ 0 & 1 & -1 \\ -1 & 0 & 1 \end{bmatrix}$ $\boldsymbol{A}_M = \begin{bmatrix} 1 & 0 & 0 & -1 & 0 & 0 \\ 0 & 1 & 0 & 0 & -1 & 0 \\ 0 & 0 & 1 & 0 & 0 & -1 \end{bmatrix}$	$\boldsymbol{s}_{sw} = \begin{bmatrix} u_{11} \\ u_{12} \\ u_{13} \\ u_{21} \\ u_{22} \\ u_{23} \end{bmatrix}$ or $\boldsymbol{s}_{sw} = \begin{bmatrix} u_{11} \\ u_{12} \\ u_{2"1"} \\ u_{22} \\ u_{31} \\ u_{32} \end{bmatrix}$	$v_s = \boldsymbol{v}_g^T \boldsymbol{A}_L \boldsymbol{u}$ $\boldsymbol{u} = \boldsymbol{A}_M \boldsymbol{s}_{sw}$ $\boldsymbol{A}_L = \boldsymbol{E}$ $\boldsymbol{A}_M = \begin{bmatrix} 1 & -1 & 0 & 0 & 0 & 0 \\ 0 & 0 & 1 & -1 & 0 & 0 \\ 0 & 0 & 0 & 0 & 1 & -1 \end{bmatrix}$

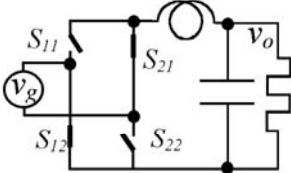**Table 2.** Structures and mathematical models of DC-to-DC converters.

Converter substructure	Converter mathematical model	
Buck structure	$$\frac{dv_o}{dt} = \frac{i_L}{C} - \frac{v_o}{RC}$$ $$\frac{di_L}{dt} = \frac{V_g}{L}u - \frac{v_o}{L}$$ $$u = \boldsymbol{A}_M \boldsymbol{s}_{sw}$$	$$\frac{dv_o}{dt} = f_v(i_L, v_o)$$ $$\frac{di_L}{dt} = f_i(v_o) + b(V_g)u$$
Boost structure	$$\frac{dv_o}{dt} = \frac{i_L}{C}(1-u) - \frac{v_o}{RC}$$ $$\frac{di_L}{dt} = \frac{V_g}{L} - \frac{v_o}{L}(1-u)$$ $$u = \boldsymbol{A}_M \boldsymbol{s}_{sw}$$	$$\frac{dv_o}{dt} = f_v(i_L, v_o) + b_1(i_L)u$$ $$\frac{di_L}{dt} = f_i(v_o, V_g) + b_2(v_o)u$$

switch position having either two isolated power storage elements (L and C) or a power filter (L,C) connected to the power source. These facts are reflected in the mathematical description of the converters: buck structures being represented in regular form [5] (system is split in the blocks so the first block has the same dimension as control and the second block does not explicitly depend on control input) (see Fig. 2.a). Boost converter have control entering both equations as depicted in Fig. 2.b. These features are common for converters with depicted position of the switching matrix independent on the number of input and output lines of the switching matrix.
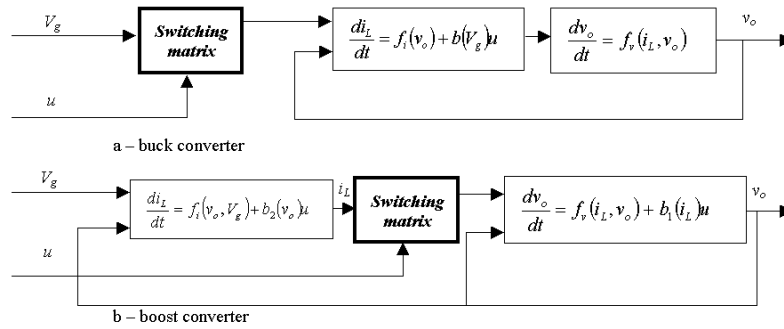
Fig. 2. Dynamical structure of: a) buck converters and b) boost converters.

Dynamics of single phase DC-to-AC and AC-to-DC converters. The
dynamics of converters with alternative voltage or current sources connected
to either input or output side of the switching matrix is the same as for
DC-to-DC converters as illustrated in Table 3. The only difference is in the
values that control could take being from discrete set $S3 = \{-1, 0, 1\}$ for
these converters and from discrete set $S2 = \{0, 1\}$ for DC-to-DC converters.
This allows to regard a DC-to-AC converter as a structure in which the load
is connected between two DC-to-DC converters.

Table 3. Structures and mathematical models of single-phase converters.
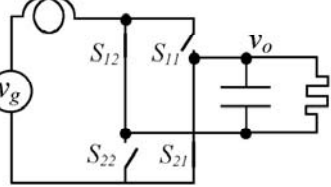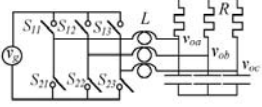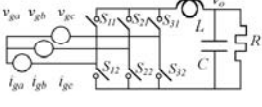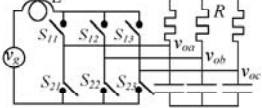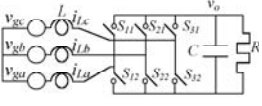
Converter substructure	Converter mathematical model
	$\dfrac{dv_o}{dt} = \dfrac{i_L}{C} - \dfrac{v_o}{RC}$ $\dfrac{di_L}{dt} = \dfrac{V_g}{L}u - \dfrac{v_o}{L}$ $u = \boldsymbol{A}_M \boldsymbol{s}_{sw}$
	$\dfrac{dv_o}{dt} = \dfrac{i_L}{C}u - \dfrac{v_o}{RC}$ $\dfrac{di_L}{dt} = \dfrac{V_g}{L} - \dfrac{v_o}{L}u$ $u = \boldsymbol{A}_M \boldsymbol{s}_{sw}$

Dynamics of three phase converters. The switching matrix for all three
phase converters DC-to-AC (inverters) and AC-to-DC (rectifiers) is the same.
Buck and boost structures for both inverters and rectifiers could easily be
recognised for three phase converters as clearly shown in Table 4. In our
analysis balanced three phase systems is assumed which can be described
in different frames of references: stationary three-phase (a, b, c), orthogonal
two-phase (α, β) and synchronous frame of references (d, q). Mapping be-
tween these frames of references is defined by matrix $\boldsymbol{A}_{abc}^{\alpha\beta}$ for (a, b, c) to
(α, β) and for $\boldsymbol{A}_{\alpha\beta}^{dq}$ to (d, q). In Table 4 mathematical models are presented
in a synchronous frame of references with θ_r as angular position of the se-
lected orthogonal frame of references. Matrix $\boldsymbol{F}(\theta_r) = \boldsymbol{A}_{\alpha\beta}^{dq}\boldsymbol{A}_{abc}^{\alpha\beta}$ is defining
the nonlinear transformation between three phase (a, b, c) and synchronous
orthogonal (d, q) frames of references. The (d, q) frame of references is de-
termined in such a way that it is synchronous with the three-phase side of
a converter (input side for rectifiers and output side for inverters). In the
presented models notation is used as follows: $\boldsymbol{v}_o^T = [v_{od}\ v_{oq}]$ the capacitance

Table 4. Structures and mathematical models of three-phase converters.

Converter substructure and control	Converter dynamics
$$\boldsymbol{A}_{\alpha\beta}^{dq} = \begin{bmatrix} \cos\theta_r & \sin\theta_r \\ -\sin\theta_r & \cos\theta_r \end{bmatrix}$$ $$\boldsymbol{A}_{abc}^{\alpha\beta} = \begin{bmatrix} 1 & -1/2 & -1/2 \\ 0 & \sqrt{3}/2 & -\sqrt{3}/2 \end{bmatrix}$$	$$\begin{bmatrix} \frac{dv_{od}}{dt} \\ \frac{dv_{oq}}{dt} \end{bmatrix} = \begin{bmatrix} -\frac{v_{od}}{RC} + \omega_r v_{oq} \\ -\frac{v_{oq}}{RC} - \omega_r v_{od} \end{bmatrix} + \frac{1}{C} \begin{bmatrix} 1 & 0 \\ 0 & 1 \end{bmatrix} \begin{bmatrix} i_{Ld} \\ i_{Lq} \end{bmatrix}$$ $$\begin{bmatrix} \frac{di_{Ld}}{dt} \\ \frac{di_{Lq}}{dt} \end{bmatrix} = \begin{bmatrix} -\frac{v_{od}}{L} + \omega_r i_{Lq} \\ -\frac{v_{oq}}{L} - \omega_r i_{Ld} \end{bmatrix} + \frac{V_g}{2L} \begin{bmatrix} 1 & 0 \\ 0 & 1 \end{bmatrix} \begin{bmatrix} u_d \\ u_q \end{bmatrix}$$ $$\boldsymbol{F}(\theta_r) = \boldsymbol{A}_{\alpha\beta}^{dq} \boldsymbol{A}_{abc}^{\alpha\beta}$$ $$\boldsymbol{u}_{dq} = \boldsymbol{F}(\theta_r)\boldsymbol{A}_M \boldsymbol{s}_{sw}$$
$$\boldsymbol{F}(\theta_r) = \boldsymbol{A}_{\alpha\beta}^{dq} \boldsymbol{A}_{abc}^{\alpha\beta}$$ $$\boldsymbol{u}_{dq} = \boldsymbol{F}(\theta_r)\boldsymbol{A}_M \boldsymbol{s}_{sw}$$	$$\frac{dv_{od}}{dt} = -\frac{v_o}{RC} + \frac{i_L}{C}$$ $$\begin{bmatrix} \frac{di_L}{dt} \\ i_{gq} \end{bmatrix} = \begin{bmatrix} -\frac{v_o}{L} \\ 0 \end{bmatrix} + \begin{bmatrix} \frac{V_g}{L} & 0 \\ 0 & i_L \end{bmatrix} \begin{bmatrix} u_d \\ u_q \end{bmatrix}$$ $$\boldsymbol{F}(\theta_r) = \boldsymbol{A}_{\alpha\beta}^{dq} \boldsymbol{A}_{abc}^{\alpha\beta}$$ $$\boldsymbol{u}_{dq} = \boldsymbol{F}(\theta_r)\boldsymbol{A}_M \boldsymbol{s}_{sw}$$
$$\boldsymbol{F}(\theta_r) = \boldsymbol{A}_{\alpha\beta}^{dq} \boldsymbol{A}_{abc}^{\alpha\beta}$$ $$\boldsymbol{u}_{dq} = \boldsymbol{F}(\theta_r)\boldsymbol{A}_M \boldsymbol{s}_{sw}$$	$$\begin{bmatrix} \frac{dv_{od}}{dt} \\ \frac{dv_{oq}}{dt} \end{bmatrix} = \begin{bmatrix} -\frac{v_{od}}{RC} + \omega_r v_{oq} \\ -\frac{v_{oq}}{RC} - \omega_r v_{od} \end{bmatrix} + \frac{i_L}{C} \begin{bmatrix} 1 & 0 \\ 0 & 1 \end{bmatrix} \begin{bmatrix} u_d \\ u_q \end{bmatrix}$$ $$\frac{di_L}{dt} = -\frac{v_d}{L}u_d - \frac{v_q}{L}u_q + \frac{V_g}{L}$$
$$\boldsymbol{F}(\theta_r) = \boldsymbol{A}_{\alpha\beta}^{dq} \boldsymbol{A}_{abc}^{\alpha\beta}$$ $$\boldsymbol{u}_{dq} = \boldsymbol{F}(\theta_r)\boldsymbol{A}_M \boldsymbol{s}_{sw}$$	$$\frac{dv_{od}}{dt} = -\frac{v_o}{RC} + \frac{i_{Ld}u_d + i_{Lq}u_q}{2C}$$ $$\begin{bmatrix} \frac{di_{Ld}}{dt} \\ \frac{di_{Lq}}{dt} \end{bmatrix} = \begin{bmatrix} \omega_r i_{Lq} + \frac{V_g}{L} \\ -\omega_r i_{Ld} \end{bmatrix} - \frac{v_o}{2L} \begin{bmatrix} 1 & 0 \\ 0 & 1 \end{bmatrix} \begin{bmatrix} u_d \\ u_q \end{bmatrix}$$

voltage vector, $\boldsymbol{i}_L^T = [i_{Ld} \; i_{Lq}]$ inductor current vector and $\boldsymbol{u}^T = [u_d \; u_q]$ is the control vector, V_g is amplitude of input voltage, R, L, C - converter parameters.

The above analysis shows that switching converters can be described as shown in equations (1)-(3) where for particular converter functions $\boldsymbol{f}_c(v_o, i_L)$, $\boldsymbol{f}_i(v_o, i_L)$, matrices $\boldsymbol{B}_c(i_L, V_g)$, $\boldsymbol{B}_u(i_L, V_g)$ and control $\boldsymbol{u}$ could be determined from the above tables. The DC-to-DC and DC-to-AC single phase converters are SISO systems while three-phase converters are MIMO systems with the three dimensional control vector. The relation (3) is shown for the purpose of having complete definition of the control input in the (d, q) frame of references.

Buck structure	Boost structure	
$\dfrac{d\boldsymbol{v}_o}{dt} = \boldsymbol{f}_c(v_o, i_L)$ $\dfrac{d\boldsymbol{i}_L}{dt} = \boldsymbol{f}_i(v_o, i_L) + \boldsymbol{B}_u(i_L, V_g)\boldsymbol{u}$	$\dfrac{d\boldsymbol{v}_o}{dt} = \boldsymbol{f}_c(v_o, i_L) + \boldsymbol{B}_c(i_L, V_g)\boldsymbol{u}$ $\dfrac{d\boldsymbol{i}_L}{dt} = \boldsymbol{f}_i(v_o, i_L) + \boldsymbol{B}_u(i_L, V_g)\boldsymbol{u}$	(1)
$\boldsymbol{u}_{sw} = \boldsymbol{A}_M \boldsymbol{s}_{sw} = \boldsymbol{u}$		(2)
$\boldsymbol{F}(\theta_r) = \boldsymbol{A}_{\alpha\beta}^{dq} \, \boldsymbol{A}_{abc}^{\alpha\beta}, \quad \boldsymbol{u}_{dq} = \boldsymbol{F}(\theta_r)\boldsymbol{A}_M \boldsymbol{s}_{sw}$ $\boldsymbol{A}_{\alpha\beta}^{dq} = \begin{bmatrix} \cos\theta_r & \sin\theta_r \\ -\sin\theta_r & \cos\theta_r \end{bmatrix}, \quad \boldsymbol{A}_{abc}^{\alpha\beta} = \begin{bmatrix} 1 & -1/2 & -1/2 \\ 0 & \sqrt{3}/2 & -\sqrt{3}/2 \end{bmatrix}$		(3)

Dynamics of electrical machines. To realise necessary power flow a switching converter (or at least a switching matrix) must be inserted between the source and a machine. Since the electrical subsystem of machines are modelled as predominantly inductive, the voltage source shall be used at the source side of the switching matrix. Mathematical models of the most common machines connected to a switching matrix are shown in Table 5. Mechanical motion is the same for all rotating machines and is described as a second order system with electromagnetic torque as the input. The electromagnetic subsystem depends on the magnetic circuitry of the particular machine and can be described by a simple first order equation for DC machines, by a second order system for PM machines and by a fourth order system for induction machines. Descriptions of the electromagnetic subsystem of a machine in Table 5 are presented in (d, q) synchronous orthogonal frame of references with orientation for all of the machines under consideration along the rotor flux vector (so called field orientation). The notation is

Table 5. Structure and mathematical models of common electrical machines

Dynamics of electromagnetic system
DC machine supplied from DC source
$\dfrac{di_q}{dt} = -\dfrac{R}{L}i_q - \dfrac{K_e}{L}\omega + \dfrac{V_g}{L}u_q\,, \qquad u = \boldsymbol{A}_M \boldsymbol{s}_{sw}$
DC machine supplied from three-phase source
$\dfrac{di_q}{dt} = -\dfrac{R}{L}i_q - \dfrac{K_e}{L}\omega + \dfrac{V_g}{L}u_q\,, \qquad \boldsymbol{u} = \boldsymbol{F}(\theta_r)\boldsymbol{A}_M \boldsymbol{s}_{sw}$ $i_q(\text{machine}) = i_d(\text{converter})\,, \qquad i_q(\text{converter}) = i_d(\text{machine})(\text{power factor})$
PM three-phase machine supplied from DC source
$\begin{bmatrix} \frac{di_d}{dt} \\ \frac{di_q}{dt} \end{bmatrix} = \begin{bmatrix} -\frac{R}{L}i_d - \omega i_q \\ -\frac{R}{L}i_q - \omega i_d - \frac{K_e}{L}\omega \end{bmatrix} + \begin{bmatrix} \frac{1}{L} & 0 \\ 0 & \frac{1}{L} \end{bmatrix} \begin{bmatrix} u_d \\ u_q \end{bmatrix}\,, \qquad \boldsymbol{u} = \boldsymbol{F}(\theta_r)\boldsymbol{A}_M \boldsymbol{s}_{sw}$
Induction machine supplied from DC source
$\begin{bmatrix} \frac{di_d}{dt} \\ \frac{di_q}{dt} \end{bmatrix} = \begin{bmatrix} -a_1 i_d + a_3\omega_r\Psi_q - a_2\Psi_d \\ -a_1 i_q - a_3\omega_r\Psi_d + a_2\Psi_q \end{bmatrix} + \begin{bmatrix} K_{id} & 0 \\ 0 & K_{idq} \end{bmatrix} \begin{bmatrix} u_d \\ u_q \end{bmatrix}; \quad \boldsymbol{u} = \boldsymbol{F}(\theta_r)\boldsymbol{A}_M \boldsymbol{s}_{sw}$ $\begin{bmatrix} \frac{d\Psi_d}{dt} \\ \frac{d\Psi_q}{dt} \end{bmatrix} = \begin{bmatrix} -\omega\Psi_q & -a_4\Psi_d \\ a_4\Psi_d & \omega\Psi_d \end{bmatrix} + \begin{bmatrix} K_\Psi & 0 \\ 0 K_\Psi \end{bmatrix} \begin{bmatrix} i_d \\ u i_q \end{bmatrix}; \quad \begin{array}{l} K_{id} = K_{iq} = \frac{1}{\sigma_m L_s} \\ K_\Psi = \frac{R_r}{L_r}L_m \end{array}$ $a_1 = \dfrac{1}{\sigma_m L_s}\left(R_s + R_r(\dfrac{L_m}{L_r})^2\right)\,, \quad a_2 = \dfrac{R_r}{\sigma_m L_s}(\dfrac{L_m}{L_r})^2\,, \quad a_3 = \dfrac{L_m}{\sigma_m L_s L_r}\,,$ $a_4 = \dfrac{R_r}{L_r}\,, \quad \sigma_m = 1 - \dfrac{L_m}{L_s L_r}$
Dynamics of mechanical subsystem for all machines
$\begin{bmatrix} \frac{d\theta}{dt} \\ \frac{d\omega}{dt} \end{bmatrix} = \begin{bmatrix} \omega \\ -\frac{T_L(\theta,\omega,t)}{J} \end{bmatrix} + \begin{bmatrix} 0 \\ K_T(i_d) \end{bmatrix} i_q$

as follows: θ, ω angular position and speed of machine, $\boldsymbol{\Psi}^T = [\Psi_d\ \Psi_q]$ is rotor flux vector; $\boldsymbol{i}^T = [i_d\ i_q]$ is stator current vector; $\boldsymbol{u}^T = [u_d\ u_q]$ is the control vector; V_g is amplitude of input voltage; J is moment of inertia; $T_L(\theta, \omega, t)$ is load torque; $K_T(i_d)$ is torque coefficient which depends on the d-component of stator current; $K_e,\ K_{iq},\ K_{id},\ K_\Psi$ are coefficients depending of the machine parameters and flux, R_r ,R_s are rotor and stator resistance, L_r ,L_s are rotor
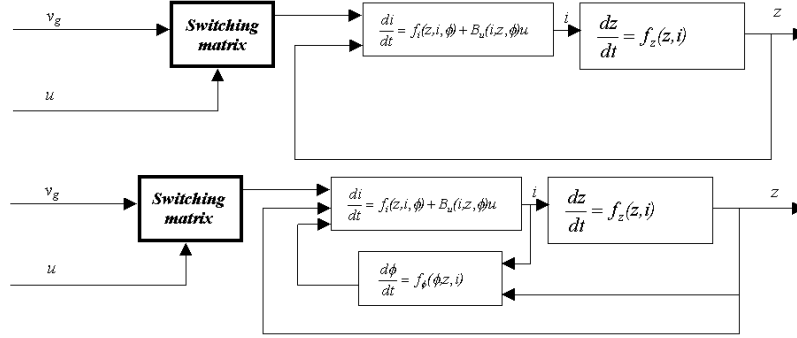
Fig. 3. Dynamical structure of electrical machines: a) DC machines and b) induction three phase machines.

and stator inductance, L_m mutual inductance, σ_m leakage factor. For a DC machine supplied from a three-phase rectifier the selection of the dq frame is related to supply voltage and is reflected in the change of the d and q coordinates in comparison with dc machine supplied from the DC source. A model of a DC machine is given for machines without field winding.

The dynamical structure of a machines is presented in Fig. 3. The difference among DC and AC machines is in the structure of the switching matrix and thus the dimensionality of the control input. For an induction machine, the dynamics of the rotor flux, with currents as input and rotor flux vector as output, should be added to the structure. A mathematical model similar to the one describing buck switching power converters could be used to describe the dynamics of electrical machines [7]

$$\frac{d\boldsymbol{i}_{dq}}{dt} = \boldsymbol{f}_i(\boldsymbol{z}, \boldsymbol{i}_{dq}, \boldsymbol{\Psi}) + \boldsymbol{B}_u(\boldsymbol{i}_{dq}, \boldsymbol{z}, \boldsymbol{\Psi})\boldsymbol{u},$$
$$\frac{d\boldsymbol{z}}{dt} = \boldsymbol{f}_z(\boldsymbol{z}, \boldsymbol{i}_{dq}); \quad \frac{d\boldsymbol{\Psi}}{dt} = \boldsymbol{f}_\phi(\boldsymbol{\Psi}, \boldsymbol{z}, \boldsymbol{i}_{dq}). \tag{4}$$

The elements of vector z are the angular position and the angular velocity of the machine. The third equation describing the change of the rotor flux is present only for the induction machine. The control input for DC machines supplied through DC-to-DC or single-phase converters is scalar. If the DC machine is supplied from a three phase source than the control input is the same as for three phase rectifiers and three phase inverters and it has the form as given in (5):

$$\boldsymbol{u}_{dq} = \boldsymbol{F}(\theta_r)\boldsymbol{A}_M \boldsymbol{s}_{sw},$$
$$\boldsymbol{F}(\theta_r) = \begin{bmatrix} \cos\theta_r & \sin\theta_r \\ -\sin\theta_r & \cos\theta_r \end{bmatrix} \begin{bmatrix} 1 & -1/2 & -1/2 \\ 0 & \sqrt{3}/2 & -\sqrt{3}/2 \end{bmatrix}, \tag{5}$$

where θ_r is the position of the synchronous frame of reference.

3   Control of power converters and electrical machines

The goal of the control system design of switching converters, in most of the practical cases, is reduced to the requirement that the output voltage of the converter tracks its reference while satisfying certain dynamical constrains (overshoot, load rejection etc.). The same is true for electrical machines for which the control goal could be stated as the requirement to have tracking in the torque, or velocity or angular position. In the following sections the unified approach to the control of switching converters and electrical machines based on the introduction of sliding mode in the control system will be shown. First we will briefly discuss some results in sliding mode design applicable to switching converters and electrical machines control.

3.1   Some results in sliding mode control

Variable structure systems are originally defined for dynamic systems described by ordinary differential equations with a discontinuous right hand side. In such a system so-called sliding mode motion can result. This motion is represented by the state trajectories in the sliding mode manifold and high frequency changes in the control. For sliding mode applications the equations of motion and the existence conditions are two basic questions to be discussed. Since models of switching converters and electrical machines are linear with respect to control further analysis will be restricted to the systems defined in the following form

$$\dot{\boldsymbol{x}} = \boldsymbol{f}(\boldsymbol{x},t) + \boldsymbol{B}(\boldsymbol{x},t)\boldsymbol{u}\,, \tag{6}$$

where $\boldsymbol{B}(\boldsymbol{x},t)$ is an $n \times m$ matrix, $\boldsymbol{x} \in \mathcal{R}^n$, $\boldsymbol{u} \in \mathcal{R}^m$. For such a system boundary-layer regularisation [1],[9] enables the substantiation of the so-called equivalent control method. In accordance with this method, in (6) control should be replaced by the equivalent control, which is the solution to $\dot{\boldsymbol{\sigma}} = \boldsymbol{G}\boldsymbol{f}(\boldsymbol{x},t) + \boldsymbol{G}\boldsymbol{B}(\boldsymbol{x},t)\boldsymbol{u}_{eq} = \boldsymbol{0}$, $\boldsymbol{G} = \{\partial\boldsymbol{\sigma}/\partial\boldsymbol{x}\}$, where $\sigma = 0$, $\sigma \in \mathcal{R}^m$ is defining sliding mode manifold while $\sigma_i = 0$ describe the so-called switching surfaces. For $\det\boldsymbol{G}\boldsymbol{B} \neq 0$ equivalent control is $\boldsymbol{u}_{eq} = -(\boldsymbol{G}\boldsymbol{B})^{-1}\boldsymbol{G}\boldsymbol{f}$, the sliding mode equation in the manifold $\sigma = 0$ is

$$\dot{\boldsymbol{x}} = \left(\boldsymbol{E} - (\boldsymbol{G}\boldsymbol{B})^{-1}\boldsymbol{G}\right)\boldsymbol{f}, \ \ \boldsymbol{\sigma} = \boldsymbol{0}\,. \tag{7}$$

From $\boldsymbol{\sigma} = \boldsymbol{0}$, m components $\boldsymbol{x}_2 \in \mathcal{R}^m$ of the state vector $\boldsymbol{x}$ may be found as a function of the rest $(n-m)$ components $\boldsymbol{x}_1 \in \mathcal{R}^{n-m}$ as $\boldsymbol{x}_2 = -\boldsymbol{\sigma}_0(\boldsymbol{x}_1)$, $\boldsymbol{\sigma}_0 \in \mathcal{R}^m$ and the order of the sliding mode equation (7) may be reduced by m:

$$\dot{\boldsymbol{x}} = \boldsymbol{f}_1\left(\boldsymbol{x}_1, -\boldsymbol{\sigma}_0(\boldsymbol{x}_1)\right), \ \ \boldsymbol{f}_1 \in \mathcal{R}^{n-m}\,. \tag{8}$$

For a system subject to disturbances $\boldsymbol{h}(\boldsymbol{x},t)$ it has been shown [17] that if $\boldsymbol{h}(\boldsymbol{x},t) \in \mathrm{range}\boldsymbol{B}$ the sliding mode motion is independent of the disturbance $\boldsymbol{h}(\boldsymbol{x},t)$ [7].

To derive the sliding mode existence conditions in analytical form the stability of the projection of the system motion on subspace $\boldsymbol{\sigma}$

$$\dot{\boldsymbol{\sigma}} = \boldsymbol{G}\boldsymbol{f}(\boldsymbol{x},t) + \boldsymbol{G}\boldsymbol{B}(\boldsymbol{x},t)\boldsymbol{u} \qquad (9)$$

should be analysed. If $\boldsymbol{G}\boldsymbol{B}$ is an identity matrix system (9) is decomposed on m first order systems and selecting the control such that signs of each component σ_i and its derivative are opposite the sliding mode motion will occur in each discontinuity surface. Other procedures and selection of the Lyapunov functions for VSS are discussed in details in [1]. The most interesting fact is that the Lyapunov function affirming the convergence to the sliding mode manifold is finite function of time. It vanishes after the finite time interval testifying that sliding mode motion arises in a finite time instant. Sliding mode equations (8) and existence conditions constitute the basis for the variety of design procedures in VSS. To demonstrate some of the design procedures, let us write system (6), subject to disturbance $\boldsymbol{D}\boldsymbol{h} = \boldsymbol{B}\boldsymbol{\lambda}$, in the so-called regular form

$$\dot{\boldsymbol{x}}_1 = \boldsymbol{f}_1(\boldsymbol{x}_1, \boldsymbol{x}_2),$$
$$\dot{\boldsymbol{x}}_2 = \boldsymbol{f}_2(\boldsymbol{x}_1, \boldsymbol{x}_2) + \boldsymbol{B}_2\boldsymbol{u} + \boldsymbol{B}_2\boldsymbol{\lambda}, \qquad (10)$$

where $\boldsymbol{x}_1 \in \mathcal{R}^{n-m}$, $\boldsymbol{x}_2 \in \mathcal{R}^m$, $\boldsymbol{f}_1(\boldsymbol{x}_1, \boldsymbol{x}_2)$, and $\boldsymbol{f}_2(\boldsymbol{x}_1, \boldsymbol{x}_2)$ are vectors of appropriate dimensions and rank$\boldsymbol{B}_2$ = rank$\boldsymbol{B}$ = m. Assume that the sliding mode manifold is defined as $\boldsymbol{\sigma} = \boldsymbol{\sigma}_0(\boldsymbol{x}_1) + \boldsymbol{x}_2 = 0$, $\boldsymbol{\sigma} \in \mathcal{R}^m$. Then the equivalent control is expressed as $\boldsymbol{u}_{eq} = -\boldsymbol{B}_2^{-1}\left(\boldsymbol{G}_1\boldsymbol{f}_1(\boldsymbol{x}_1, \boldsymbol{x}_2) + \boldsymbol{f}_1(\boldsymbol{x}_1, \boldsymbol{x}_2)\right) - \boldsymbol{\lambda}$. It depends on disturbance and in most cases its realization is unpractical. Calculating $(\boldsymbol{u} + \boldsymbol{\lambda})$ from $d\boldsymbol{\sigma}/dt = \boldsymbol{0}$ and substituting it to second equations in (10) then, when the sliding mode appears in this manifold, the system behaviour is governed by the $(n - m)$ order equation

$$\dot{\boldsymbol{x}}_1 = \boldsymbol{f}_1\left(\boldsymbol{x}_1, -\boldsymbol{\sigma}_0(\boldsymbol{x}_1)\right), \quad \boldsymbol{x}_2 = -\boldsymbol{\sigma}_0(\boldsymbol{x}_1). \qquad (11)$$

In (11) vector $\boldsymbol{\sigma}_0(\boldsymbol{x}_1)$ could be treated as "virtual control" and should be selected to satisfy the desired system dynamics. For control input selection the projection of the system motion on m-dimensional space $\boldsymbol{\sigma}$ is found

$$\dot{\boldsymbol{\sigma}} = \boldsymbol{f}(\boldsymbol{x}_1, \boldsymbol{x}_2, \boldsymbol{\lambda}) + \boldsymbol{B}_2\boldsymbol{u}, \quad \boldsymbol{f} \in \mathcal{R}^m,$$
$$\boldsymbol{f}(\boldsymbol{x}_1, \boldsymbol{x}_2, \boldsymbol{\lambda}) = \boldsymbol{G}_1\boldsymbol{f}_1 + \boldsymbol{f}_2\boldsymbol{x}_2 + \boldsymbol{B}_2\boldsymbol{\lambda}. \qquad (12)$$

The discontinuous control $\boldsymbol{u} = -\boldsymbol{B}_2^{-1}M\text{sign}(\boldsymbol{\sigma})$, $M = \text{const.} > 0$ leads to

$$\dot{\sigma}_i = f_i(\boldsymbol{x}_1, \boldsymbol{x}_2, \boldsymbol{\lambda}) - Mu_i, \quad i = 1, ..., m. \qquad (13)$$

There exists large enough $M > 0$ such that the functions σ_i, $i = 1, ..., m$ and derivatives $\dot{\sigma}_i$ have opposite signs, sliding mode will occur in each of the discontinuity surfaces.

Discrete time sliding mode was introduced for discrete time plants [11],[13],[15]. The most significant difference with the continuous time sliding mode is that

motion in the sliding mode manifold may occur in discrete time systems with continuous right hand side By applying the sample and hold process with sampling period T, and integrating the solution over interval $t \in [kT, (k+1)T]$ with $\boldsymbol{u}(t) = \boldsymbol{u}(kT)$ and $\boldsymbol{d}(t) = \boldsymbol{d}(kT)$, the discrete time model of plant (6) may be represented as

$$\boldsymbol{x}_{k+1} = \boldsymbol{F}_k \boldsymbol{x}_k + \bar{\boldsymbol{B}} \boldsymbol{u}_k + \boldsymbol{P} \boldsymbol{d}_k \,. \tag{14}$$

The sliding manifold is defined as $\boldsymbol{\sigma}_k = \boldsymbol{G} \boldsymbol{x}_k$, $k = 1, 2,$. In [11] the equivalent control $\boldsymbol{u}_k^{eq} = \boldsymbol{u}_k^{eq}(kT)$ is defined as the solution of

$$\boldsymbol{\sigma}_{k+1} = \boldsymbol{G} \boldsymbol{x}_{k+1} = \boldsymbol{G} \boldsymbol{F}_k \boldsymbol{x}_k + \boldsymbol{G} \bar{\boldsymbol{B}} \boldsymbol{u}_k^{eq} + \boldsymbol{G} \boldsymbol{P} \boldsymbol{d}_k = \boldsymbol{0} \,. \tag{15}$$

Provided that $\det \boldsymbol{G} \bar{\boldsymbol{B}} \neq 0$ the equivalent control can be expressed as

$$\boldsymbol{u}_k^{eq} = -(\boldsymbol{G} \bar{\boldsymbol{B}})^{-1} \boldsymbol{G} (\boldsymbol{F}_k \boldsymbol{x}_k + \boldsymbol{P} \boldsymbol{d}_k) \,. \tag{16}$$

It is important to note that matching conditions now are defined in terms of matrices $\boldsymbol{G}$, $\bar{\boldsymbol{B}}$, $\boldsymbol{P}$. The required magnitude of control (16) may be large and limitation should be applied, so the final form of the control is

$$\boldsymbol{u}_k^{eq} = \begin{cases} -(\boldsymbol{G} \bar{\boldsymbol{B}})^{-1} \boldsymbol{G} (\boldsymbol{F}_k \boldsymbol{x}_k + \boldsymbol{P} \boldsymbol{d}_k^*), & \text{if } |\boldsymbol{u}_k| < U_o \\ -U_o \text{sign}(\boldsymbol{\sigma}_k), & \text{if } |\boldsymbol{u}_k| \geq U_o \end{cases} \,, \tag{17}$$

where $\boldsymbol{d}_k^*$ is the estimated disturbance and U_o is a control input bound. In another approach for system (6) asymptotic stability of the solution $\boldsymbol{\sigma}(\boldsymbol{x}) = \boldsymbol{0}$ can be assured if one can find a control input such that the stability criteria are satisfied for the following Lyapunov function $\nu = \boldsymbol{\sigma}^T \boldsymbol{\sigma}/2$ with the requirement that the time derivative $(d\nu/dt)$ has a certain form, for example $d\nu/dt = -\boldsymbol{\sigma}^T \boldsymbol{D} \boldsymbol{\sigma}$, $\boldsymbol{D} > \boldsymbol{0}$, [16]. Then the control input, with sampling interval T, that satisfy the given requirements is in the form

$$\boldsymbol{u}_k = \boldsymbol{u}_{k-1} - (\boldsymbol{G} \boldsymbol{B} T)^{-1} \left((\boldsymbol{E} + T \boldsymbol{D}) \boldsymbol{\sigma}_k - \boldsymbol{\sigma}_{k-1} \right) \,. \tag{18}$$

The realisation of control (18) requires information on the sliding functions and the plant gain matrix, which is much easier to obtain than information necessary to implement algorithm (17).

Mathematical models of the switching converters and electrical machines could be presented in regular form (10) with discontinuous control influencing the change of the currents and currents being treated as "virtual control" in the voltage dynamics (for converters) or mechanical motion dynamics (for machines). The structure of the boost converters is more complicated with control entering all the equations of the system. Despite the differences in the dynamical structure the control system design for buck and boost converters and electrical machines may follow the two-step procedure:

- Select control $\boldsymbol{u}$ such that inductor current (or electromagnetic torque in electrical machines) tracks its reference;

- Select the current reference (virtual control) so that capacitance voltage (or mechanical coordinates) satisfy prescribed dynamical behaviour.

This procedure is not so obvious for the boost structures since control enters both equations. In the framework of sliding mode systems the above procedure for boost converters requires substitution of the equivalent control to the first equation and then taking current reference as "virtual control" input. In the following sections we will show the consequent application of the above procedure in details without presenting unnecessary details for particular converters or machines.

3.2   Control of DC-to-DC converters and DC machines

In this section the control of DC-to-DC converters and DC machines both having scalar control input is discussed. Control of DC machines supplied from three-phase sources will be discussed in the section dealing with control of three-phase converters and AC machines.

Control of DC-to-DC buck converter. Assume the current reference as continuous function $i_L^{ref}(t)$ then, for the tracking error $\sigma = i_L^{ref}(t) - i_L(t)$ and the control selected as $u = (1 - \text{sign}\sigma)/2$ the sliding mode exists if the equivalent control $0 \leq u_{eq} \leq 1$ is calculated as:

$$\frac{d\sigma}{dt} = \frac{d(i_L^{ref} - i_L)}{dt} = \frac{di_L^{ref}}{dt} + \frac{v_o}{L} - \frac{V_g}{L}u_{eq} = 0$$

$$\Rightarrow u_{eq} = \frac{1}{V_g}(L\frac{di_L^{ref}}{dt} + v_o). \tag{19}$$

Substituting the equivalent control to the original equations of the system one can obtain:

$$\frac{dv_o}{dt} = \frac{i_L^{ref}}{C} - \frac{v_o}{RC}; \;\; i_L(t) = i_L^{ref}(t). \tag{20}$$

From (20) reference current could be selected using well-established design procedures for linear systems. For example, if the first order response $\sigma_v = \rho(v_o^{ref} - v_o) + d(v_o^{ref} - v_o)/dt = 0$ of closed loop system is required, the reference current could be easily determined as

$$i_L^{ref} = \text{sat}\left(\frac{v_o}{R} + \rho C(v_o^{ref} - v_o) + C\frac{dv_o^{ref}}{dt}\right) \Rightarrow i_L^{ref} = \text{sat}(i_L + C\sigma_v) \tag{21}$$

where $\text{sat}(\bullet)$ is the saturation function. Structure of system (21) is shown in Fig. 4. Another structure of the control system may be determined from the required closed loop dynamics by inserting $dv_o/dt = i_L/C - v_o/RC$ into the expression for σ_v which leads to $\sigma_v = \rho(v_o^{ref} - v_o) + dv_o^{ref}/dt + v_o/RC - i_L/C =$
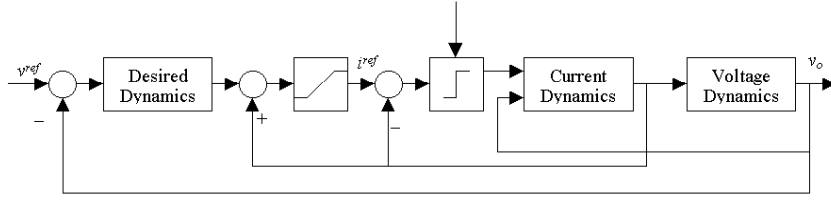
Fig. 4. Structure of the converter control system.

$(i_L^{ref} - i_L)/C$ and selecting the control as $u = (1 - \text{sign}(C\sigma_v))/2$ the sliding mode motion is established in manifold $\sigma_v = 0$ if $0 \le u_{eq} \le 1$ and the same result is obtained as in algorithm (21).

The structure in Fig. 4 is suitable for the implementation of different control algorithms in designing the reference current, thus it leaves more room for merging other control techniques with the sliding mode. This will be especially clear in the control of the boost type of power converters.

Control of DC machines. By following the same procedure as for buck converters the DC machine tracking error could be defined as $\sigma = i_q^{ref}(t) - i_q(t)$ with the control $u = (1 - \text{sign}\sigma)/2$ the sliding mode exists if the equivalent control satisfies $-1 \le u_{eq} = (L/V_g)(di_q^{ref}/dt + R/Li_q + K_e/L\omega) \le 1$. By substituting u_{eq} to the original system the motion of the Dc machine is reduced to the second order system

$$\frac{d\theta}{dt} = \omega\,; \quad \frac{d\omega}{dt} = -\frac{T_L(\theta, \omega, t)}{J} + \frac{K_T(i_d)}{J} i_q^{ref}\,. \tag{22}$$

By requiring the closed loop transient to satisfy $\sigma_\theta = C_\theta(\theta^{ref} - \theta) + C_\omega \frac{d(\theta^{ref} - \theta)}{dt} + \frac{d^2(\theta^{ref} - \theta)}{dt^2} = 0$ determined by the design parameters C_θ and C_ω the reference current becomes

$$\sigma_\theta = C_\theta(\theta^{ref} - \theta) + C_\omega \frac{d(\theta^{ref} - \theta)}{dt} + \frac{d^2(\theta^{ref} - \theta)}{dt^2} = \frac{K_T}{J}(i_q^{ref} - i_q)\,,$$

$$i_q^{ref} = \text{sat}\left(\frac{T_L}{K(i_d)} + C_\theta(\theta^{ref} - \theta) + C_\omega \frac{d(\theta^{ref} - \theta)}{dt} + \frac{d^2\theta^{ref}}{dt^2}\right)\,. \tag{23}$$

Note that for $C_\theta = 0_\omega$ the above dynamics reduces to $\sigma_\omega = C_\omega(\omega^{ref} - \omega) + C_\omega(d(\omega^{ref} - \omega)/dt) = 0$ and defines the desired dynamics for velocity control. Implementation of control (23) requires information on the machine load which could be obtained using disturbance observer techniques proposed by Ohnishi in [18]. Manipulating (23) one can determine a much more simple, way of calculating reference current

$$i_q^{ref} = \text{sat}\left(i_q + \frac{J}{K_T(i_d)}\sigma_\theta\right)\,. \tag{24}$$

Structure of the control system is the same as the one depicted in Fig. 4. These results depict earlier shown similarities between buck converters and electrical machines. The structure of the control is the same, with necessary changes in measured variables. In [22], [23] the application of the sliding mode control to DC machine combining the acceleration, the velocity and the position control is proposed. Proposed algorithm ensures robustness against parameters and disturbance changes even in the acceleration stage. Design of the sliding mode control for DC electrical machines based on the reduced order model (dynamics of the electrical current is neglected) is discussed in details in [4] and [26].

Control of boost DC-to-DC converter. Assume the current reference as the continuous function $i_L^{ref}(t)$ then, selecting tracking error $\sigma = i_L^{ref}(t) - i_L(t)$ and control $u = (1 - \mathrm{sign}\sigma)/2$ the sliding mode exists if equivalent control (25) satisfies conditions $0 \leq u_{eq} \leq 1$

$$\frac{d\sigma}{dt} = \frac{d(i_L^{ref} - i_L)}{dt} = \frac{di_L^{ref}}{dt} + \frac{v_o}{L}(1 - u_{eq}) - \frac{V_g}{L} = 0$$

$$\Rightarrow u_{eq} = \frac{1}{v_o}\left(L\frac{di_L^{ref}}{dt} + v_o - V_g\right). \tag{25}$$

By substituting u_{eq} to the original equations of the boost converter one could determine

$$\frac{C}{2}\frac{d(v_o)^2}{dt} + \frac{v_o^2}{R} = V_g i_L^{ref} - \frac{L}{2}\frac{d(i_L^{ref})^2}{dt} = (V_g - v_L)i_L^{ref}, \quad i_L = i_L^{ref}, \tag{26}$$

where v_L represents the voltage drop on the inductance L. System (26) may be interpreted as the description of power conservation in the circuit $(C/2)d(v_o)^2/dt + v_L i_L^{ref} = V_g i_L^{ref} - (v_o^2/R)$. From the control point of view it could be regarded as a linear first order system with the square of the output voltage v_o^2 as output and reference inductor current as control. With such definition of variables the mathematical description reduces to the first order system nonlinear with respect to the control. For DC-to-DC converters the change of energy stored in inductance could be neglected (average $v_L = 0$) and the system reduces to the first order linear system $(C/2)d(v_o)^2/dt + (v_o^2/R) = V_g i_L^{ref}$ and selection of the reference current may follow the same procedure as for buck converters [3],[17]. Another often applied solution is the feed-forward calculation of the reference current from the reference voltage [26].

3.3   Control of three phase converters and three phase machines

Three phase converters and electrical machines structurally differ from their DC counterparts in the number of energy storage elements and in the structure of the switching matrix. The dynamical structure of the systems remains

the same as for their DC counterparts except that the there-phase are MIMO systems. That allows conduct design of the control in the same two-step procedure as applied for dc systems.

Current control in three phase systems. For modelling and control design purposes the three phase switching matrix has been defined by the three-dimensional control vector $\boldsymbol{u} = \boldsymbol{A}_M \boldsymbol{s}_{sw}$. Vector $\boldsymbol{s}_{sw}$ has six elements but due to electric circuits constraints for buck inverter and boost rectifier, vector $\boldsymbol{s}_{sw}$ may have the following values $\boldsymbol{S}_1 = [1\,0\,0\,0\,1\,1]$, $\boldsymbol{S}_2 = [1\,1\,0\,0\,0\,1]$, $\boldsymbol{S}_3 = [0\,1\,0\,1\,0\,1]$, $\boldsymbol{S}_4 = [0\,1\,1\,1\,0\,0]$, $\boldsymbol{S}_5 = [0\,0\,1\,1\,1\,0]$, $\boldsymbol{S}_6 = [1\,0\,1\,0\,1\,0]$, $\boldsymbol{S}_7 = [1\,1\,1\,0\,0\,0]$, $\boldsymbol{S}_8 = [0\,0\,0\,1\,1\,1]$; for boost inverter and buck rectifier vector $\boldsymbol{s}_{sw}$ may have the following values $\boldsymbol{S}_1 = [1\,0\,0\,0\,0\,1]$, $\boldsymbol{S}_2 = [0\,0\,1\,0\,0\,1]$, $\boldsymbol{S}_3 = [0\,1\,1\,0\,0\,0]$, $\boldsymbol{S}_4 = [0\,1\,0\,0\,1\,0]$, $\boldsymbol{S}_5 = [0\,0\,0\,1\,1\,0]$, $\boldsymbol{S}_6 = [1\,0\,0\,1\,0\,0]$, $\boldsymbol{S}_7 = [1\,1\,0\,0\,0\,0]$, $\boldsymbol{S}_8 = [0\,0\,1\,1\,0\,0]$, $\boldsymbol{S}_9 = [0\,0\,0\,0\,1\,1]$.

For inverters and rectifiers the number of independent control inputs is three. As depicted in Fig. 5 for three-phase inverters the number of independent variables to be controlled is two: for inverters these are the d and q components of output voltage, for AC machines they are the same as the components of supply voltage. For inverters and machines supplied from DC sources there is no variable to be controlled on the input side. For three-phase rectifiers the output is the DC source and thus only one independent variable (output current or voltage) is to be controlled. On the input side of the rectifier, the magnitude of voltage or current are defined thus only phase shift between the voltage and the current vector could be controlled. This allows introduction of an additional requirement to the control system design. The
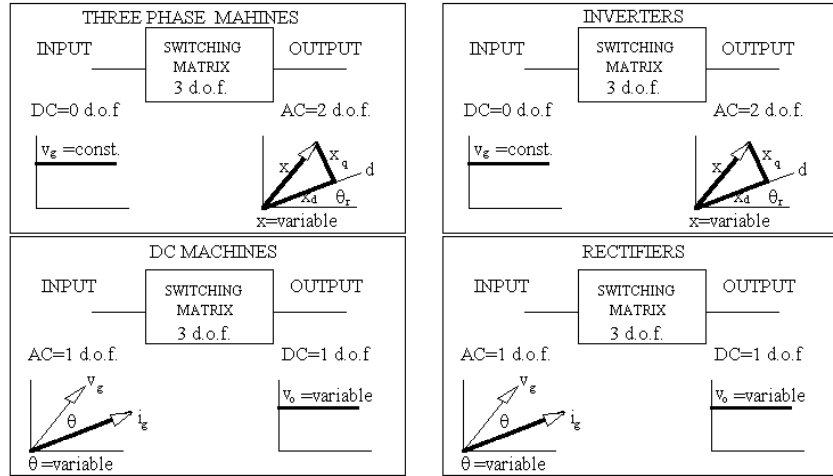

Fig. 5. The assignment of the degrees of freedom in control for three-phase switching matrix.

most natural choice is to relate this additional requirement to the selection of the switching pattern.

Let us now look at design of the switching pattern for the three phase converters in more details. Current control is based on the sliding mode existence in the manifold $\boldsymbol{\sigma}^T = [\boldsymbol{i}^{ref}(t) - \boldsymbol{i}]^T = \boldsymbol{0}$ where vector $\boldsymbol{\sigma}^T = [\sigma_d\,\sigma_q]^T$ with $\sigma_d = i_d^{ref}(t) - i_d$, $\sigma_q = i_q^{ref}(t) - i_q$ and i_d^{ref}, i_q^{ref} are continuous functions to be determined later. Design of the current controller is based on the system description (4) $d\boldsymbol{i}_{dq}/dt = \boldsymbol{f}_{idq} + \boldsymbol{B}_{udq}\boldsymbol{u}_{dq}$ where matrix $\boldsymbol{B}_{udq}$ is diagonal. The structure of function $\boldsymbol{f}_{idq}$ and matrix $\boldsymbol{B}_{udq}$ could be easily found from mathematical models given in Tables 4 and 5. The time derivative of $\boldsymbol{\sigma}^T = [\sigma_d\,\sigma_q]^T$ is determined as

$$\frac{d\boldsymbol{\sigma}}{dt} = \frac{d\boldsymbol{i}_{dq}^{ref}}{dt} - \frac{d\boldsymbol{i}_{dq}}{dt} = \frac{d\boldsymbol{i}_{dq}^{ref}}{dt}\boldsymbol{f}_{idq} - \boldsymbol{B}_{udq}\boldsymbol{u}_{dq}, \;\; \boldsymbol{u}_{dq}^T = [u_d\,u_q]\,. \tag{27}$$

Equivalent control can be calculated as $\boldsymbol{B}_{udq}^{-1}[d\boldsymbol{i}_{dq}^{ref}/dt - \boldsymbol{f}_{idq}] = \boldsymbol{u}_{eq}$ and equation (27) is expressed as

$$\frac{d\boldsymbol{\sigma}_{dq}}{dt} = \boldsymbol{B}_{udq}[\boldsymbol{u}_{eq} - \boldsymbol{u}_{dq}(S_i)], \quad i = 1, ..., 9\,. \tag{28}$$

Control vectors could take values from the discrete set $\boldsymbol{S}_8 = \{\boldsymbol{S}_1, \boldsymbol{S}_2, \boldsymbol{S}_3, \boldsymbol{S}_4, \boldsymbol{S}_5, \boldsymbol{S}_6, \boldsymbol{S}_7, \boldsymbol{S}_8, \boldsymbol{S}_9\}$ as depicted in Fig. 6.a. All realizable values of the equivalent control lie inside the hexagon spaned by the elements of the set $\boldsymbol{S}_8[7]$. The rate of change of error is proportional to the differences between the vector of equivalent control and the realisable control vectors. For a particular combination of errors all permissible vectors $\boldsymbol{S}_i$ that satisfy the sliding mode existence conditions could be determined from $(d\sigma_d/dt)\,\sigma_d < 0$ and $(d\sigma_q/dt)\,\sigma_q < 0$ or $\text{sign}(\boldsymbol{u}_{eq} - \boldsymbol{u}_{dq}(\boldsymbol{S_i})) = -\text{sign}(\boldsymbol{\sigma}_{dq})$ as shown in Fig. 6.b. For some combinations of errors there are more than one permissible vector

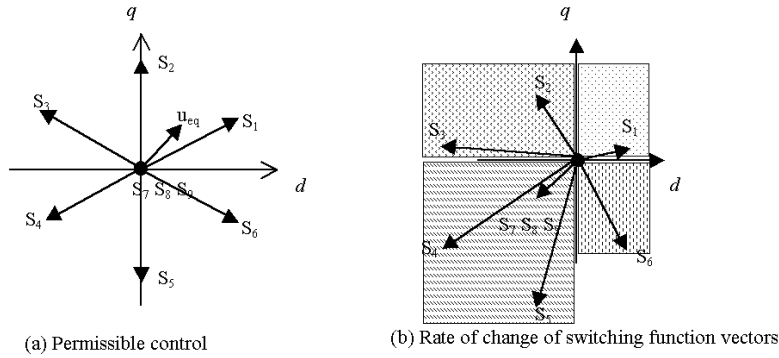(a) Permissible control   (b) Rate of change of switching function vectors

Fig. 6. Control vectors and selection of permissible control for given combination of the signs of control errors.

that leads to an ambiguous selection of the control and consequently existence of more than one solution for the selection of switching pattern .

The same could be concluded from $\operatorname{rank}\boldsymbol{F}(\theta_r) = \operatorname{rank}(\boldsymbol{A}_{\alpha\beta}^{dq}\boldsymbol{A}_{abc}^{\alpha\beta}) = 2$. Ambiguity in selection of the control vector based on selected u_d and u_q allows us to have a number of different PWM algorithms based on satisfying sliding mode conditions in (d, q) frame of references. In early works [7] the following solution was proposed: add an additional requirement $\vartheta(t) = 0$ to the control system specification so that (27) is augmented to have the form

$$\begin{bmatrix} \frac{d\boldsymbol{\sigma}_{dq}}{dt} \\ \frac{d\vartheta}{dt} \end{bmatrix} = \begin{bmatrix} \frac{d\boldsymbol{i}^{ref}}{dt} - \boldsymbol{f}_{idq} \\ \boldsymbol{f}_\vartheta \end{bmatrix} - \begin{bmatrix} \boldsymbol{B}_{udq}\boldsymbol{F}(\theta_r) \\ \boldsymbol{b}_\vartheta^T \end{bmatrix} \boldsymbol{u}(\boldsymbol{S}_i) \,, \tag{29}$$

$$\frac{d\boldsymbol{\sigma}_N}{dt} = \boldsymbol{f}_N - \boldsymbol{B}_N\boldsymbol{u}(\boldsymbol{S}_i), \quad \boldsymbol{u}^T(\boldsymbol{S}_i) = [u_a \, u_b \, u_c] \,. \tag{30}$$

Vector $\boldsymbol{b}_\vartheta$ should be selected so that $\operatorname{rank}\boldsymbol{B}_N = 3$. the simplest solution is for $\dot{\vartheta}(t) = u_a + u_b + u_c$ [7],[26] then matrix $\boldsymbol{B}_N$ will have full rank. To determine the switching pattern, the simplest way is to use the nonlinear transformation $\boldsymbol{\sigma}_s = \boldsymbol{B}_N^{-1}\boldsymbol{\sigma}_N$, then the sliding mode conditions are satisfied if the control is selected as

$$\operatorname{sign}\left(u_j(\boldsymbol{S}_i)\right) = -\operatorname{sign}(\sigma_{sj}), \quad -1 \le u_{eq} \le 1 \,. \tag{31}$$

This line of reasoning with some variations has been the most popular in designing the sliding mode based switching pattern [4],[7].

Another solution implicitly applied in most of the so-called space vector PWM algorithms is based on the simple idea [5] using transformation

$$\boldsymbol{u}_{abc} = \operatorname{rank}(\boldsymbol{A}_{\alpha\beta}^{dq}\boldsymbol{A}_{abc}^{\alpha\beta})^T\boldsymbol{u}_{dq}$$

to the (a, b, c) reference frame. Then components u_a, u_b and u_c of $\boldsymbol{u} = \boldsymbol{A}_M\boldsymbol{s}_{sw}$ are selected according to the following rule

$$S_i = \begin{cases} \operatorname{sign}(u_a(S_i)) = \operatorname{sign}(u_d\cos\theta_r - u_q\sin\theta_r) \\ \operatorname{sign}(u_b(S_i)) = \operatorname{sign}(u_d\cos(\theta_r - 2\pi/3) - u_q\sin(\theta_r - 2\pi/3)) \\ \operatorname{sign}(u_b(S_i)) = \operatorname{sign}(u_d\cos(\theta_r - 4\pi/3) - u_q\sin(\theta_r - 4\pi/3)) \end{cases}$$
$$i = (1, 2, ..., 8, 9) \,. \tag{32}$$

This idea is analysed in details in [7]. Further simplification of this algorithm leads to its implementation using a look-up table [19].In [24] and [25] the so-called space vector PWM based on the sliding mode approach is discussed. The solution is based on the expression (32) but it is realized using space sectors.

In the application of above algorithms switching is realized using hysteresis which, as follows from (28) directly determine the current ripple to be equal to the half of the hysteresis width. For the given current ripple (constant hysteresis width) the time between two switching for each component is directly proportional to $[u_{eqj} - u_{dqj}]$, $(j = d, q)$, $(i = 1, ...9)$. A new class

of the switching algorithms based on the simple requirement that control should be selected to give the minimum rate of change of control error could be designed for which the same error will be achieved with less switching effort. The algorithm can be formulated in the following form [3]

$$S_i = \begin{cases} \min \| \, \boldsymbol{u}_{eq}(t) - \boldsymbol{u}_j(S_i) \, \| \\ \mathrm{sign}\,([u_{eqd} - u_d(S_i)] \bullet \sigma_d(t)) = -1 \\ \mathrm{sign}\,([u_{eqq} - u_q(S_i)] \bullet \sigma_q(t)) = -1 \end{cases}, \quad i = (1, 2, ..., 8, 9). \tag{33}$$

The difference in behaviour for algorithm (32) and (33) is depicted in Fig. 7, where the steady state operation of buck inverter current control is shown. The operating point for both algorithms is the same and the width of hysteresis is also kept the same. The difference in the switching frequency of the voltage is easily detectable.

All of the above algorithms naturally include so-called over-modulation functionality. This can be seen in the diagrams depicted in Fig. 8. For algorithm (33) behaviour of an induction machine (P=4kVA, p=2, U=220 V) current control loop is depicted. (α, β) currents and control are shown in Fig. 8.a. for a loaded machine and wref=50p [rad/s]. Note that switching is regular between the two closest vectors and zero vector. In Fig. 8.b. the current vector is depicted for $w^{ref} = 95\pi$ [rad/s]. For this condition the sliding mode existence conditions are violated in certain regions of the plane. In Fig. 8.c. the current vector is depicted for $w^{ref} = 100\pi$ [rad/s]. For this condition the sliding mode existence conditions cannot be satisfied and the system operates under a six-step mode.

Due to the specifics of three-phase balanced systems the number of independent controls for the switching matrix is higher than the dimension of the controlled current vector This is the basic reason that three-phase PWM, under many different names, is still attractive as a research topic. The solution proposed in [15] shows that the formalization of the minimization of TDF in
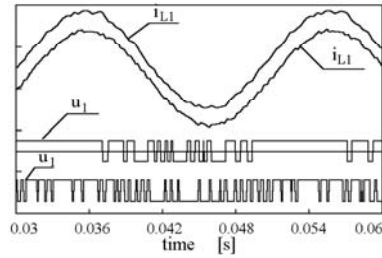

Fig. 7. The steady state operation of buck inverter current control for switching algorithms (32) - lower trace and (33) - upper trace.
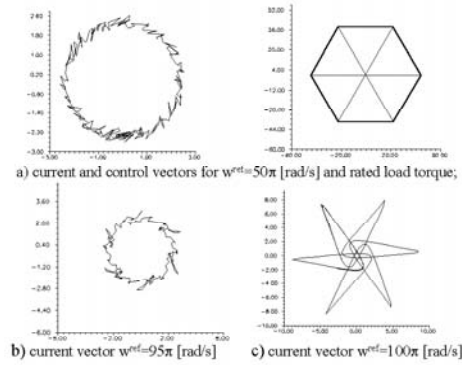

a) current and control vectors for w^{ref}=50π [rad/s] and rated load torque;

b) current vector w^{ref}=95π [rad/s]   c) current vector w^{ref}=100π [rad/s]

Fig. 8. Change of the current and control vectors in (α, β) frame of references.

the above framework has lead to a solution that is far better in comparison with other so-called space vector approaches [16].

In the sliding mode dynamics of current the control loop is reduced to $\boldsymbol{\sigma}^T = [\boldsymbol{i}^{ref}(t) - \boldsymbol{i}]^T = \boldsymbol{0}$ or $i_d^{ref}(t) = i_d$ and $i_q^{ref}(t) = i_q$ with equivalent control being determined as $\boldsymbol{B}_{udq}^{-1}[d\boldsymbol{i}^{ref}/dt - \boldsymbol{f}_{idq}] = \boldsymbol{u}_{eq}$. In order to complete the design of converters and electrical machines the reference currents shall be determined.

Voltage and mechanical motion control system design. For buck converters and electrical machines with reference currents interpreted as virtual control inputs the description could be easily transformed to the following form

$$\frac{d\boldsymbol{x}}{dt} = \boldsymbol{f}_x(\boldsymbol{x}) + \boldsymbol{B}_i(\boldsymbol{x})\boldsymbol{i}^{ref}\,, \tag{34}$$

where vector $\boldsymbol{x}^T = [x_1\ x_2]$ represent either the vector of output voltage (for converters) or the vector with velocity and position (for electrical machines).

For the buck inverter both components of the reference current could be determined from the specification of the voltage loop, but for buck rectifiers only the d-component of the source current can be determined from the voltage loop specification. The q-component of the source current does not influence the output voltage and thus represent current circulating between supply sources and creating reactive power flow from sources. The same is directly applicable for a DC machine supplied by the three-phase rectifier.

Since all machines have the same structure of mechanical subsystem the results obtained for DC machines may be directly applicable to AC machines thus giving a way of determining one component of the current vector. The other component of the current vector should be determined from the requirement of the magnetic circuits of the machine and is specific for each type of the machine. For PM and induction three-phase machines the d-component of the current defines the rotor flux so it should be selected taking rotor flux behavior into consideration.

The requirements for converters and machines are presented in Table 6. the selection of the components of the switching function vector is given along with the expression for the reference current calculation. The reference current is selected following the discrete time sliding mode control design and for all systems under consideration it is $\boldsymbol{i}_k^{ref} = \boldsymbol{i}_{k-1}^{ref} - (\boldsymbol{G}\boldsymbol{B}\boldsymbol{T})^{-1}((\boldsymbol{E}+\boldsymbol{T}\boldsymbol{D})\boldsymbol{\sigma}_k - \boldsymbol{\sigma}_{k-1})$; $\boldsymbol{G} = \{\partial\boldsymbol{\sigma}/\partial\boldsymbol{x}\}$ where T is the sampling interval. The realisation of this control algorithm requires information on the sliding functions and the plant gain matrix.

Consider the three-phase boost rectifier connected as a controllable current source as shown in Fig. 9. Its role is to generate current flow so that the energy source is loaded by active power or the reactive power of source is zero $Q_s = 0$ which gives $i_{sq}^{ref} = 0$. The d-component reference current

Table 6. The selection of desired dynamics and control vector

Type	Function σ	Reference currents
Buck rectifier	$\sigma_d = v_o^{ref} - v_o$ $\sigma_q = i_{qav}^{ref} - i_{qav}$ usually $i_{qav}^{ref} = 0$	
Dc machine	$\sigma_d = C_\theta \Delta\theta + \dfrac{d\Delta\theta}{dt};\ \ \Delta\theta = \theta^{ref} - \theta$ $\sigma_q = i_{qav}^{ref} - i_{qav}$ usually $i_{qav}^{ref} = 0$	
Buck inverter	$\sigma_d = v_{od}^{ref} - v_{od}$ $\sigma_q = v_{oq}^{ref} - v_{oq}$	$\boldsymbol{i}_k^{ref} = \boldsymbol{i}_{k-1}^{ref} - (\boldsymbol{GB}T)^{-1}$ $(\ (\boldsymbol{E} + T\boldsymbol{D})\boldsymbol{\sigma}_k - \boldsymbol{\sigma}_{k-1});$ $\boldsymbol{G} = \{\partial\boldsymbol{\sigma}/\partial\boldsymbol{x}\}$
PM synchronous machine	$\sigma_d = i_{dav}^{ref} - i_{dav}$ usually $i_{dav}^{ref} = 0$ $\sigma_q = C_\theta \Delta\theta + \dfrac{d\Delta\theta}{dt};\ \ \Delta\theta = \theta^{ref} - \theta$	$\boldsymbol{i}_{dq}^{ref} = [i_d^{ref}\ i_q^{ref}]^T$ $\boldsymbol{\sigma}_{dq}^{ref} = [\sigma_d\ \sigma_q]^T$
Induction machine	$\sigma_d = \sigma_\phi(\phi, \phi^{ref}) = \Delta\phi;$ $\Delta\phi = \phi^{ref} - \phi$ $\sigma_q = C_\theta \Delta\theta + \dfrac{d\Delta\theta}{dt};\ \ \Delta\theta = \theta^{ref} - \theta$	
Boost rectifier	$\sigma_d = \mu\left((v_o^{ref})^2 - (v_o)^2\right)$ $\sigma_q = i_{qav}^{ref} - i_{qav}$ usually $i_{qav}^{ref} = 0$	

shall be determined from the capacitance voltage. It is easy to show that $(C/2)\,(dv_{od}^2/dt) + v_{od}^2/R = V_g i_d^{ref} - v_L i_d^{ref}$ which is the same as for the DC-to-DC boost converter and all comments regarding the DC-to-DC boost converter control are applicable.

The structure of the power converters and electrical machines system can be presented as in Fig. 10. where the current control loop operates in sliding mode with discontinuous control. The structure is the same as one shown in Fig. 4. with additional details on the outer loop controller. The selected structure is only one of the several possible solutions, other structures may be derived by applying some other design procedures many of which are developed in the framework of motion control systems. By doing so, essential features of the sliding mode are preserved by current loop design.
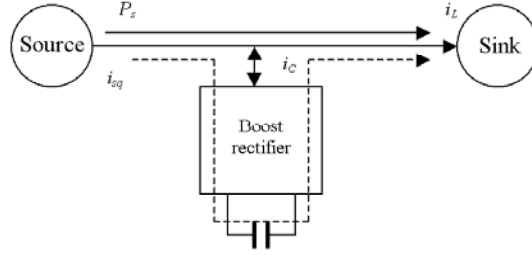
Fig. 9. Power flow in system when boost converter is used as an active power filter.
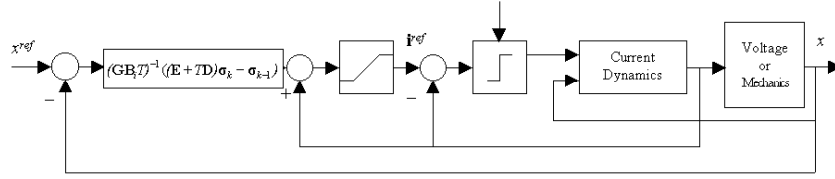

Fig. 10. Structure of the converters and electrical machine control system.

Application of the above algorithms requires information on currents and voltages for converters and mechanical coordinates for electrical machines. Usually measurement of electrical quantities is not considered demanding so realization of the control algorithms in the case of switching converters does not represent any problem. This may not be true for AC electrical machines and especially for the induction machine. For these machines the synchronous frame of references is determined by the rotor flux vector, which is not accessible for measurement and should be derived using observer. Since induction machine is a nonlinear system the observer design may not be so straight forward a task. In the section 4 of this paper we will be discussing the sliding mode based observers of induction machine rotor flux and velocity.

4   Induction machine observer

Design of a IM sensorless drives is still a challenge. The basic problem is speed estimation especially at the low speed range and under light load conditions. In this section the VSS approach to rotor flux and speed estimation of an induction machine will be discussed.

The description of the machine in the (α, β) frame of references is

$$\frac{d\boldsymbol{\Psi}_r}{dt} = -\boldsymbol{B}_r\boldsymbol{\Psi}_r + \frac{R_r L_m}{L_r}\boldsymbol{i}_s; \quad \boldsymbol{B}_r = \begin{bmatrix} \frac{R_r}{L_r} & -\omega \\ \omega & \frac{R_r}{L_r} \end{bmatrix}, \tag{35}$$

$$\frac{d\boldsymbol{i}_s}{dt} = \frac{1}{\sigma L_s}\left(\frac{L_m}{L_r}\left(-\boldsymbol{B}_r\boldsymbol{\Psi}_r + \frac{R_r L_m}{L_r}\boldsymbol{i}_s \right) - R_s\boldsymbol{i}_s + \boldsymbol{u}_s \right). \tag{36}$$

Formally it is possible to design a stator current observer based on voltage and current measurements and with a rotor flux vector derivative as the control input:

$$\frac{d\hat{\boldsymbol{i}}_s}{dt} = \frac{1}{\sigma L_s}\left(-\frac{L_m}{L_r}\boldsymbol{u}_\Psi - R_s\hat{\boldsymbol{i}}_s + \boldsymbol{u}_s\right). \tag{37}$$

This selection of the observer control input is different from the usually used current error feedback (well known Gopinath's method), application of sliding mode control based on current feedback [17], or selecting the unknown velocity as the control input [18],[4],[26].

The estimation error is determined as

$$\frac{d\boldsymbol{\varepsilon}_i}{dt} = \frac{d(\boldsymbol{i}_s - \hat{\boldsymbol{i}}_s)}{dt} = \frac{1}{\sigma L_s}\left(\frac{L_m}{L_r}\left(\left(-\boldsymbol{B}_r\boldsymbol{\Psi}_r + \frac{R_r L_m}{L_r}\boldsymbol{i}_s\right) + \boldsymbol{u}_\Psi\right) - R_s\boldsymbol{\varepsilon}_i\right) \tag{38}$$

If the sliding mode exists then from $d\boldsymbol{\varepsilon}_i/dt = \boldsymbol{0}$, and $\boldsymbol{\varepsilon}_i = \boldsymbol{0}$. Under the assumption that the angular velocity is known, from (38) one can find

$$\hat{\boldsymbol{\Psi}}_r = \boldsymbol{B}_r^{-1}\left(\boldsymbol{u}_{\Psi eq} - \frac{R_r L_m}{L_r}\boldsymbol{i}_s\right). \tag{39}$$

In the observer design suitable for the sensorless drive, the observer control input should be a known function of the motor speed so that, after establishing sliding mode in current tracking loop, the speed can be determined as a unique solution. This leads to the following selection of the structure of the stator current observer

$$\frac{d\hat{\boldsymbol{i}}_s}{dt} = \frac{1}{\sigma L_s}\left(\frac{L_m}{L_r}\left(-\boldsymbol{u}_\phi + \frac{R_r L_m}{L_r}\hat{\boldsymbol{i}}_s\right) - R_s\hat{\boldsymbol{i}}_s + \boldsymbol{u}_s\right) \tag{40}$$

and the estimation error becomes:

$$\frac{d\boldsymbol{\varepsilon}_i}{dt} = \frac{d(\boldsymbol{i}_s - \hat{\boldsymbol{i}}_s)}{dt} = \frac{1}{\sigma L_s}\left(\frac{L_m}{L_r}\left(-\boldsymbol{B}_r\boldsymbol{\Psi}_r + \boldsymbol{u}_\phi\right) - \left(R_s + \frac{R_r L_m^2}{L_r^2}\right)\boldsymbol{\varepsilon}_i\right) \tag{41}$$

Algorithm (18) could be used to calculate the control $\boldsymbol{u}_{\phi k} = \boldsymbol{u}_{\phi k-1} + (\sigma L_s L_r / L_m T)((1 + \rho T)\boldsymbol{\varepsilon}_{ik} - \boldsymbol{\varepsilon}_{ik-1})$ with $\boldsymbol{\varepsilon}_i = [\varepsilon_{i\alpha}\ \varepsilon_{i\beta}]$. From $d\boldsymbol{\varepsilon}_i/dt = \boldsymbol{0}$ the equivalent control is determined as $\boldsymbol{u}_{\phi eq} = \boldsymbol{B}_r\boldsymbol{\Psi}_r$. The rotor flux observer could be selected as having the same structure as (35) with the additional convergence term $\boldsymbol{f}$ whose structure will be explained later

$$\frac{d\hat{\boldsymbol{\Psi}}_r}{dt} = -\boldsymbol{u}_\phi + \frac{R_r L_m}{L_r}\hat{\boldsymbol{i}}_s + \boldsymbol{f}. \tag{42}$$

Now flux estimation error can be calculated as:

$$\frac{d\boldsymbol{\varepsilon}_\Psi}{dt} = \frac{d(\boldsymbol{\Psi}_r - \hat{\boldsymbol{\Psi}}_r)}{dt} = -\boldsymbol{B}_r\boldsymbol{\Psi}_r + \boldsymbol{u}_\phi + \frac{R_r L_m}{L_r}\boldsymbol{i}_s - \boldsymbol{f}. \tag{43}$$

To ensure convergence $\boldsymbol{f}$ could be selected in the following form:

$$\boldsymbol{f} = \boldsymbol{k}\hat{\boldsymbol{\varepsilon}}_{\Psi}\,, \tag{44}$$

where

$$\begin{bmatrix} \bar{\varepsilon}_{\Psi\alpha} \\ \bar{\varepsilon}_{\Psi\beta} \end{bmatrix} = \begin{bmatrix} \hat{\Psi}_{\alpha} & -\hat{\Psi}_{\beta} \\ \hat{\Psi}_{\beta} & \hat{\Psi}_{\alpha} \end{bmatrix} \begin{bmatrix} \mu \\ \eta \end{bmatrix}, \quad \mu = \frac{\Delta\hat{x}_r\,\hat{x}_r + \Delta\hat{\omega}\,\omega}{\hat{\omega}^2 + \hat{x}_r^2}, \quad \eta = \frac{\Delta\hat{x}_r\,\hat{\omega} - \Delta\hat{\omega}\,\hat{x}_r}{\hat{\omega}^2 + \hat{x}_r^2},$$

and

$$\begin{bmatrix} \hat{\omega} \\ \hat{x}_r \end{bmatrix} = \frac{1}{\parallel \hat{\Psi}_r \parallel^2} \begin{bmatrix} \hat{\Psi}_{\beta} & -\hat{\Psi}_{\alpha} \\ \hat{\Psi}_{\alpha} & \hat{\Psi}_{\beta} \end{bmatrix} \begin{bmatrix} u_{\phi\alpha} \\ u_{\phi\beta} \end{bmatrix}, \tag{45}$$

$$\begin{bmatrix} \Delta\hat{\omega} \\ \Delta\hat{x}_r \end{bmatrix} = \frac{\sigma_m L_s L_r}{L_m T} \begin{bmatrix} \hat{\Psi}_{\alpha} & -\hat{\Psi}_{\beta} \\ \hat{\Psi}_{\beta} & \hat{\Psi}_{\alpha} \end{bmatrix} \left(\rho\varepsilon_i + \frac{d\varepsilon_i}{dt} \right). \tag{46}$$

If the sliding mode in the current control loop (41) exists and both $\Delta\hat{\omega} = 0$ and $\Delta\hat{x}_r = 0$, then $\mu = 0$ and $\eta = 0$ and consequently $\hat{\boldsymbol{\varepsilon}}_{\Psi} = \boldsymbol{0}$. The convergence of the observer is easier to analyse by projecting errors in the (d, q) frame of references as given by (47)

$$\begin{bmatrix} e_d \\ e_q \end{bmatrix} = \begin{bmatrix} \hat{\Psi}_{\alpha} & -\hat{\Psi}_{\beta} \\ \hat{\Psi}_{\beta} & \hat{\Psi}_{\alpha} \end{bmatrix} \begin{bmatrix} \varepsilon_{\Psi\alpha} \\ \varepsilon_{\Psi\beta} \end{bmatrix}. \tag{47}$$

After some algebra one can find

$$\begin{bmatrix} \frac{de_d}{dt} \\ \frac{de_q}{dt} \end{bmatrix} = -\begin{bmatrix} -k & T_e + \hat{\omega} \\ T_e - \hat{\omega} & -k \end{bmatrix} \begin{bmatrix} e_d \\ e_q \end{bmatrix} + k \parallel \Psi \parallel \begin{bmatrix} \mu \\ \eta \end{bmatrix}. \tag{48}$$

The design parameter k could be selected from (48) so that the estimated rotor flux tends to its real value. T_e denotes the electromagnetic torque of the machine.

5   Neural network application in sliding mode systems

As an example of the application of the above ideas in this section a neural network controller for the induction machine will be discussed [21]. The procedure below is valid for all converters and electrical machines since all of them could be presented in the form (34). The structure of the system with a neural network controller is depicted in Fig. 11. For system (34) and the sliding mode manifold selected as given in Table 6. The equivalent control could be determined as $\boldsymbol{i}_{eq}^{ref} = -(\boldsymbol{GB}_i)^{-1}(\boldsymbol{Gf}_x)$. In the system of Fig. 11 the neural network is used to determine the unknown part of equivalent control in the system. The control input could be expressed as

$$\boldsymbol{i}^{ref} = -(\boldsymbol{GB}_i)^{-1}(\boldsymbol{GN}(\boldsymbol{x}, t)) - (\boldsymbol{GB}_i)^{-1}\boldsymbol{D}\boldsymbol{\sigma}\,, \tag{49}$$
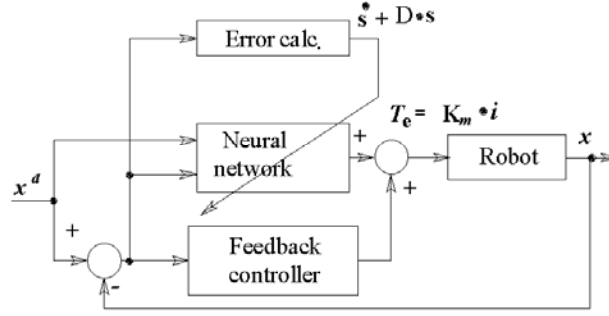
Fig. 11. The structure of the control system.

where $\boldsymbol{GN}(\boldsymbol{x}, t)$ is the output of the neural network. This control input gives the time derivative of the Lyapunov function candidate $V = \boldsymbol{\sigma}^T \boldsymbol{\sigma}/2$ as [20]

$$\frac{dV}{dt} = \boldsymbol{\sigma}^T \frac{d\boldsymbol{\sigma}}{dt} = \boldsymbol{\sigma}^T \left(\boldsymbol{G}(\boldsymbol{f}_x - \boldsymbol{N}(\boldsymbol{x},t)) \right) - \boldsymbol{\sigma}^T \boldsymbol{D}\boldsymbol{\sigma} \,. \tag{50}$$

The stability conditions will be satisfied if $\parallel \boldsymbol{\sigma}^T \boldsymbol{G}(\boldsymbol{f}_x - \boldsymbol{N}(\boldsymbol{x},t)) \parallel < \parallel \boldsymbol{\sigma}^T \boldsymbol{D}\boldsymbol{\sigma} \parallel$ holds, in other words if neural network is trained to make zero the error function $\boldsymbol{Z} = \boldsymbol{G}(\boldsymbol{f}(\boldsymbol{x},t) - \boldsymbol{N}(\boldsymbol{x},t)) = \boldsymbol{D}\boldsymbol{\sigma} + \dot{\boldsymbol{\sigma}}$. This means that the neural network approximation error could be calculated from the sliding mode function. An obvious selection of the role of the neural network is to minimise

$$\Gamma = \frac{1}{2}\boldsymbol{Z}^T \boldsymbol{Z} = \frac{1}{2}(\boldsymbol{D}\boldsymbol{\sigma} + \dot{\boldsymbol{\sigma}})^T (\boldsymbol{D}\boldsymbol{\sigma} + \dot{\boldsymbol{\sigma}}) \tag{51}$$

thus to assure mapping $\boldsymbol{GN} \to \boldsymbol{Gf}$. An important feature of the developed scheme is that the approximation error is available on-line. It is important to notice that the feedback controller assures the stability of the overall system. Assume neural network model

$$y_i^l = g_i^l \left(\sum_{j=1}^{k} w_{ij}^l a_j^l + b_i^l \right), \;\; g_i^l(net_i^l) = \tanh(net_i^l) = \frac{2}{1 + e^{-2net_i^l}} - 1 \,,$$

where a_j^l is the j-th input of the l-th layer, y_i^l is the output of the i-th neuron in the l-th layer, w_{ij}^l is the weight connecting the j-th input and the i-th neuron in the l-th layer and b_i^l is the bias of the i-th neuron in the l-th layer of the neural network. Learning proceeds using a gradient descent where η denotes the learning rate $\Delta w_{ij}^l = -\eta \, \partial E / \partial w_{ij}^l$. For the output layer, denoted by L, the following equations can be used:

$$\frac{\partial \Gamma}{\partial y_i^{L-l}} = \boldsymbol{G}(\boldsymbol{f}_x - \boldsymbol{N}(\boldsymbol{x}))(-g_m) \,, \tag{52}$$

$$\Delta w_{ij}^L = \eta g_m (\boldsymbol{D}\boldsymbol{\sigma} + \dot{\boldsymbol{\sigma}}) g^l(a_i^L) y_j^L \,. \tag{53}$$
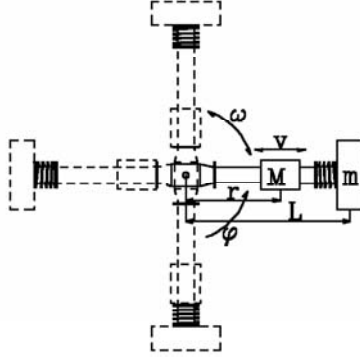
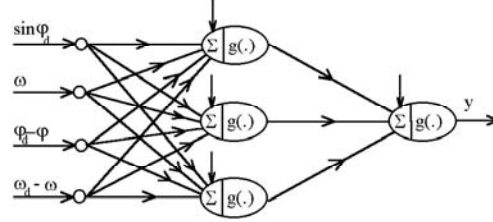**Fig. 12.** Experimental system.

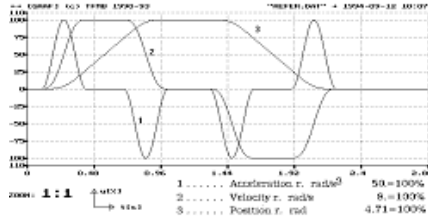**Fig. 13.** The structure of the neural network.

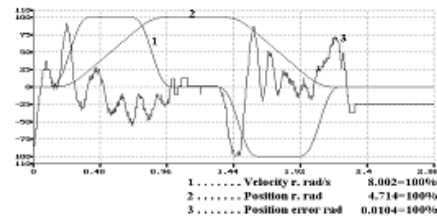**Fig. 14.** Desired values of position, velocity and acceleration.

Fig. 15. Experimental results for performing task presented in Fig. 14.

For the hidden layer a back-propagation learning algorithm as is used with $\Delta w_{ij}^l = \eta\,\delta_j^l\,y_j^l$.

The mechanism featured in Fig. 12 was used in the experiment [21]. A hammer, mounted on the axis of the induction motor was used and a mass - spring - damper load was added to show effects of coupling. The two layered neural network used as an on-line estimator is featured in Fig. 13. φ_d is the desired position and ω_d is the desired velocity of the system. The system task was to learn to perform the operation, described in Fig. 14. Movement is performed using the so-called sin^2 shaped acceleration. The results are depicted in Fig. 15, and good tracking performance is obtained.

6   Conclusions

A unified approach to control system design for switching converters and electrical machines is discussed. It has been shown that, due to the structural similarities, switching power converters and electrical machines could be analysed in the same framework and the control system structure is the same for both classes of the plant. The switching matrix plays the role of a control element, introducing change in the structure of the system and, thus

making design in the framework of variable structure systems and sliding mode control a natural choice. Engineering methods rather than historical overview of published results is presented. As an example of the possibility of combining neural networks and VSS approaches the induction machine neural network controller is discussed. Due to the appropriate selection of the system's error the learning procedure has been determined so that it does not require any measurements except those needed for the sliding mode function calculation. This error signal has been used for the gradient descent algorithm. Theoretical results have been confirmed by experiments on IM loaded with a nonlinear load.

References

1. Utkin, V. I.,(1992) *Sliding modes in control and optimization*, Springer-Verlag.
2. Wood, P., (1981) *Switching Power Converters*, Van Nostrand Reinholh.
3. Šabanović, N., Ohnishi, K. and Šabanović, A., (1992) "Sliding Modes Control of Three Phase Switching Converters," Proc of IECON'92 Conference, 319-325, San Diego, USA.
4. Utkin, V. I., (1993) "Sliding Mode Control Design Principles and Applications to Electric Drives", *IEEE Tran. Ind. Electr.* Vol. 40, No.1, 421-434.
5. Luk'yanov, A.G. and Utkin, V. I., (1991) "Methods of reducing equations of dynamic systems to a regular form," *Aut. Remote Control*, Vol. 42, No.12, 413-420.
6. Šabanović, A., Izosimov, D.B., (1981) "Application of sliding mode to induction motor control," *IEEE Trans. Ind. Aut.* Vol. IA 17 No.1, 41-49.
7. Drazenovic B., (1969) "The invariance conditions in variable structure systems", *Automatica,* Vol.5, 287-295, Pergamon Press.
8. Drakunov, S. V. and Utkin, V. I., (1989) "On discrete-time sliding modes", Proc. of Nonlinear control system design Conf., 273-278, Capri, Italy.
9. Furuta K., (1990) "Sliding mode control of a discrete system", *System and Control letters,* Vol. 14, No. 2, 145-152.
10. Utkin, V.I., (1993) "Sliding Mode Control in Discrete Time and Difference Systems", Variable Structure and Lyapunov Control, Ed. by Zinober A.S., Springer Verlag, London.
11. Šabanović, A., (1992) "Sliding modes in motion control systems", Proc. of $2^n d$ IEEE Intl. Workshop on advanced motion control, 150-156, Nagoya, Japan.
12. Venkataramana, R., Sabanovic, A. and Cuk, S., (1985) " Sliding Mode Control of DC-to-DC Converters," Proc. of IECON'85, San Francisco, USA.
13. Ohnishi , K. and Murakami, T., (1989) "Application of Advanced Control Techniques in Electrical Drives", Proc. of IEEE Conf. on Microcomputer Control of Electric Drives, Trieste, Italy.
14. Šabanović, N., Šabanović, A. and Ninomiya, T., (1994) "PWM in Three-Phase Switching Converters - Sliding Mode Solution", Power Electronics Specialist Conference PESC'94, Taipei, Taiwan.
15. Chen, Y., Fujikawa, K., Kobayashi, H., Ohnishi, K. and Sabanovic, A., (1997) "Direct Instantaneous Distorsion Minimization Control for Three Phase Converter," *Tran. IEEJ,* Vol. 117-D, No. 7, (in Japanese).